

Available online at [www.sciencedirect.com](http://www.sciencedirect.com)**ScienceDirect**

Procedia Engineering 105 (2015) 323 – 328

**Procedia  
Engineering**[www.elsevier.com/locate/procedia](http://www.elsevier.com/locate/procedia)

6th BSME International Conference on Thermal Engineering (ICTE 2014)

## Bio-inspired design: aerodynamics of boxfish

Andrei Kozlov, Harun Chowdhury\*, Israt Mustary, Bavin Loganathan and Firoz Alam

*School of Aerospace, Mechanical and Manufacturing Engineering, RMIT University, Melbourne, 3083, Australia*

---

### Abstract

This paper investigates the aerodynamic behavior of a boxfish using both experimental and computational methods. A scaled up model boxfish was manufactured and tested in RMIT Industrial Wind Tunnel under a range of Reynolds numbers and yaw angles. The drag, lift and side forces and their corresponding moments were measured simultaneously. A CAD model of the boxfish was used in CFX FLUENT Computational Fluid Dynamics (CFD) modeling. The CFD modeling data were validated using the experimental findings. The results indicate that the drag coefficient of a boxfish is around 0.10 which is significantly lower than current drag coefficient of a passenger car. Hence, a boxfish shape can be adapted for achieving low drag and energy efficient motor vehicle design.

© 2015 The Authors. Published by Elsevier Ltd. This is an open access article under the CC BY-NC-ND license (<http://creativecommons.org/licenses/by-nc-nd/4.0/>).

Peer-review under responsibility of organizing committee of the 6th BSME International Conference on Thermal Engineering (ICTE 2014)

**Keywords:** Passenger car; aerodynamic drag; box fish; wind tunnel; yaw angle; CFD.

---

### 1. Introduction

The concept of Biomimicry refers to the study and observation of how nature has been dealing with problems it has faced over at least 600 million years and applying it to human problems [1-2]. The concept itself is relatively new and only recent problems humanity has been facing, such as global warming, has been inspiring vehicle designers and aerodynamicists to explore a new ways of aerodynamic drag reduction. Due to only a recent

---

\* Corresponding author. Tel.: +61 3 99256103; fax: +61 3 99256108.  
E-mail address: [harun.chowdhury@rmit.edu.au](mailto:harun.chowdhury@rmit.edu.au)

emergence of biomimicry, there is no real procedure which defines how the process of biomimicry should be applied to vehicle aerodynamic problems. The following steps have been thought out to allow for an initial step of implementation of biologically inspired design process into vehicle aerodynamics.

According to European Regulations, the CO<sub>2</sub> emission from a new vehicle in 2012 cannot be exceeded by 120 grams per kilometer and in 2020 this figure should be limited to 95 grams per kilometer [3]. Additionally, stiff market competition and rising fuel price force vehicle manufacturers to develop fuel efficient vehicles to be competitive and economically viable. One way to develop fuel efficient vehicles is the reduction of aerodynamic drag as it accounts for around 80% of the total drag at vehicle cruising speeds over 80 km/h [4]. The reduced drag will not only lower the fuel consumption but also the CO<sub>2</sub> emissions. The major drag reductions have been achieved by optimizing vehicle exterior body shapes over four decades. Further reduction can affect the vehicle styling – an important factor for customer perception (aesthetics) and marketing. The aerodynamic efficiency is more important for electric road vehicles due to the need of extension of operational range. Until recently road vehicle designs have been designed purely based on visual appreciation. Nature has been dealing with such problems for at least 600 million years and very often there is an optimized solution to a problem it has faced [1]. It is therefore evident that each evolution stage should be more efficient than the previous. Therefore, it should be beneficial for designers and aerodynamicist to choose nature as a mentor, and observe how previously nature has dealt with a problem, such as efficient propulsion through a medium.

The traditional box shape passenger cars in 1920s started to become more streamlined in 1960-70s as aerodynamics became a dominant factor to reduce the fuel consumption especially during the 1973-74 oil embargo by OPEC. The aerodynamic efficiency indicator (drag coefficient) started to fall from around 0.60 for a typical passenger car in 1960s to 0.40 in late 1970s and 0.28 in 2012. Further drag reduction in passenger cars is hard to achieve using already streamlined body shapes. Slight reduction in drag coefficient is still possible if smooth under body, smart wheel, reduced wheel wells and convoy driving (platooning) are used. However, the smooth under body, wheels and wheel arches deteriorate vehicle cooling performance. Therefore, an alternative body shape with lower drag coefficient is paramount. Despite having unpleasant appearance, the boxfish is considered to have lower aerodynamic resistance than dolphins and penguins. Thanks to its large cross section and structural rigidity, the boxfish is more suited to mimic in automobile body shapes. Some car manufacturers including Daimler-Chrysler are attempting to replicate the boxfish shape into their car designs. However, scant information is currently available in the public domain on boxfish aerodynamics. Therefore, the main objective of this study is to investigate the aerodynamic behavior of a boxfish using both experimental and computational methods.

### Nomenclature

$F_D$	aerodynamic drag (N)
$C_D$	aerodynamic drag coefficient
$Re$	Reynolds number
$V$	wind velocity (m/s)
$\mu$	absolute dynamic viscosity of wind (Pa)
$\rho$	air density (kg/m <sup>3</sup> )
$A$	projected frontal area of boxfish (m <sup>2</sup> )

## 2. Methodology

### 2.1. Selection of a model

One problem with the integration of biomimicry with vehicle aerodynamics is the compatibility of a suitable model, which can be used and replicated. Very often the process of reduction in aerodynamic/hydrodynamic drag involves the reduction of frontal area which is encountered by the flow. This is very commonly seen in fish, as they tend to generally be long and slim as seen in a presentation by Choi [5], which reduces the pressure drag. They also have unique skin surfaces to reduce the associated skin friction. Such geometries are however not of much use for

mimicking in vehicle aerodynamics. However, this does not apply to all species. In fact, many species in the Ostraciidae fish family have very unique body geometries. Many of these fish from Ostraciidae are optimized for benefits other than hydrodynamic drag and are not suited to be used as a model. One example is the Horn-Nosed boxfish, captured by Randall [6]. Although it belongs to the same family, its extra “horn” like front is not desired in vehicle design. However, the yellow boxfish has a very simple box geometry without any additional geometric features which is desired for vehicle replication. Therefore, a yellow boxfish shape has been selected to study its aerodynamic behavior especially drag using both computational fluid dynamics (CFD) modeling and wind tunnel experimental study.

## 2.2. CFD modeling and wind tunnel testing

Modern CFD modeling techniques together with increasing computational capabilities are becoming much more of a viable tool to model various shapes including road vehicles. It also offers an alternative tool to costly wind tunnel experimentation. However, the wind tunnel data is still required to validate the CFD modeling findings. For the experimental study, the RMIT Industrial Wind Tunnel was used. It is a closed return circuit with a rectangular test section of 6 m<sup>2</sup> (3 m wide, 2 m high and 9 m long). The maximum speed of the wind in the test section is approximately 145 km/h. More details about the tunnel can be found in Alam et al. [7]. A physical model of simplified boxfish was designed and manufactured. The model was made of Styrofoam. A device was developed to hold the model with a 6-component force sensor (made by JR3 Inc., USA) to measure all 3 forces (drag, side and lift/down forces) and 3 moments (yaw, roll and pitch) simultaneously. The aerodynamic drag forces were measured over a range of wind speeds (20 to 100 km/h with an increment of 10 km/h). The drag forces were converted to non dimensional parameter drag coefficient ( $C_D$ ). The aerodynamic drag coefficient ( $C_D$ ) and the Reynolds number ( $Re$ ) are defined as:

$$C_D = \frac{D}{\frac{1}{2} \rho V^2 A} \quad (1)$$

$$Re = \frac{\rho V d}{\mu} \quad (2)$$

The lift and side forces and their coefficients were not determined and presented in this paper. Only drag data is presented here.

The CFX (version 14.5) was used to model the airflow around the model. A CAD model was developed using CATIA. Two turbulence schemes (standard  $k-\omega$  and  $k-\epsilon$ ) were used to model the flow around the CAD model. Preparation of the simplified boxfish model for CFD modeling was accomplished through the process of mimicry. A specific yellow boxfish was used as a baseline for the simplified model as shown in Fig 1(a). The simplification involved the idealization of the boxfish model from the real yellow boxfish with addition of idealization in order to create the model. The idealization of the model was most noticeable at the front and rear where the mouth and tail regions of the fish are located. These were idealized and incorporated to the main body which was replicated as accurately as was possible. Due to the file conversion process, careful attention was devoted to achieving a CFD model which was as close to CAD model as possible, which was achieved through a selected conversion settings. Once the model was incorporated into the idealized wind tunnel test section in CFD domain, the wind tunnel atmosphere was modeled by incorporating the stationary simplified boxfish model. For the Reynolds number sensitivity tests, the wind tunnel environment was halved as seen in Fig. 4 due to symmetry, which allowed much faster simulation times to be achieved, as well as allow further local mesh refinement in close proximity to the simplified boxfish model. For comparison, the tests were also replicated with full size wind tunnel geometry. The wind tunnel model and setup is shown in Fig. 1(b).

The methodology of all computational work utilizes a hybrid mesh consisting of unstructured triangular and tetrahedral mesh, throughout the entire volume of the wind tunnel environment. An additional layer in the region of

surface of the boxfish model with finer surface mesh is added in order to more correctly predict the flow separation and flow phenomena in close proximity to the boxfish model. Furthermore, a box of influence is added to the wind tunnel environment, in order to effectively distribute finer mesh to the region where flow phenomena must be more accurately evaluated, the meshing setup for the Reynolds number sensitivity tests can be seen in Fig. 2. A similar approach is used for the yaw test. The box of influence has a much greater concentration of mesh, thereby greatly reducing any unnecessary flow evaluation and simulation time in regions further away from the sides of the boxfish model.

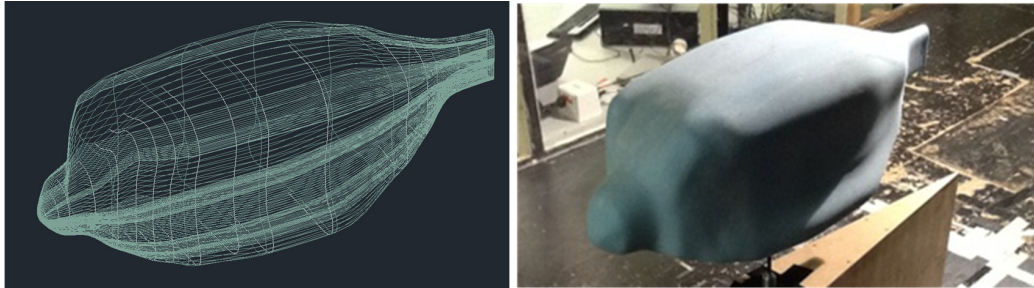


Fig. 1. (a) computational model; (b) wind tunnel model.

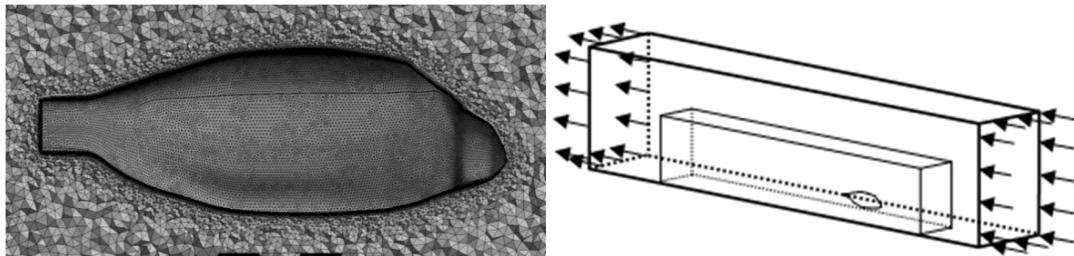


Fig. 2. (a) generated mesh for boxfish model; (b) schematic setup of half model tests.

In order to satisfy all requirements of both turbulence models, different meshing approaches were made for both the inflation layer and box of influence, in the case of  $k-\omega$ , the mesh was reduced in order to minimize the mesh size increase as much as possible, due to the small first layer height required to achieve the desired  $y^+$  for the turbulence model. The settings used for both turbulence models and respective meshes are summarized in Table 1, and the setup in Fig. 2(b).

Table 1. Meshing summary for non yaw tests.

	$k-\varepsilon$	$k-\omega$
Surface element size	25 ( mm )	0.025
Inflation setting	First aspect ratio ( scalable wall function )	First layer thickness (automatic wall function )
Maximum number of layer	5	50 ( 30 )
First aspect ratio	5	-
First layer height	-	0.004 ( mm )
$Y^+$ ( typical )	29 - 65	0.012 – 1.6

Two tests for  $k-\omega$  were completed; one is classified as a stable and the other as non-stable. Due to the known instability of the turbulence model/common convergence issues, the non-stable case is that which the residuals are isolating between a value of  $10^{-3}$  and a stable case in which all residuals isolate in close proximity to  $10^{-5}$  however do not meet the convergence target of  $10^{-5}$  which was set for both turbulence model cases. However, in all tests, the drag convergence was prioritized before residual convergence. The fluid and boundary properties for both CFD modeling are shown in Table 2.

Table 2. Boundary conditions and fluid properties.

Boundary properties	
Inlet wind speed	20, 40, 60, 80 and 100 km/h
Outlet wind speed	Average static pressure = 0
Wind tunnel walls	All symmetry
Model wall	No slip wall
Fluid property	Air at 25 °C ( isothermal )

### 3. Results and discussion

Fig. 3(a) shows the drag coefficient convergence characteristics of the simplified boxfish model for the standard  $k-\epsilon$  turbulence model. All tests were conducted for inflow velocities of 20–100 km/h which equate to the corresponding Reynolds number as seen in Fig. 3. From Fig. 3(a), a clear convergence was observed as the mesh was refined to 8 million elements, it was important to achieve this convergence to increase the confidence of obtaining a correct result based on the selected turbulence model. Like satisfying  $y^+$  requirements for the turbulence model used, it was important to achieve this convergence to the maximum available computational mesh quantity, which was around 9 million elements of unstructured mesh. Fig. 3(b) shows the variation between the described stable case (50 layers) and non-stable case (30 layers) as well as  $k-\epsilon$  and currently available wind tunnel data. From Fig. 3(b), the varying difference of prediction between both turbulence models was noted. At lower  $Re$  numbers,  $k-\epsilon$  was found to under predict where as  $k-\omega$  over predicted  $C_D$ , however there are some doubts of the accuracy of the wind tunnel used for lower  $Re$  numbers. For most cases  $k-\omega$  predicted the results slightly better than  $k-\epsilon$ , however due to its large computational time, it was less efficient when comparing the accuracy/simulation time of the two turbulence models used. It was found that the wind tunnel data also more closely match the less stable  $k-\omega$  case, which had not fully converged to the 10-5 residual target, during which the  $C_D$  had also been slightly more unstable. Due to the high likelihood of wind tunnel inconsistencies and equipment errors/limits, it could explain the higher drag readings for most  $Re$  number cases.

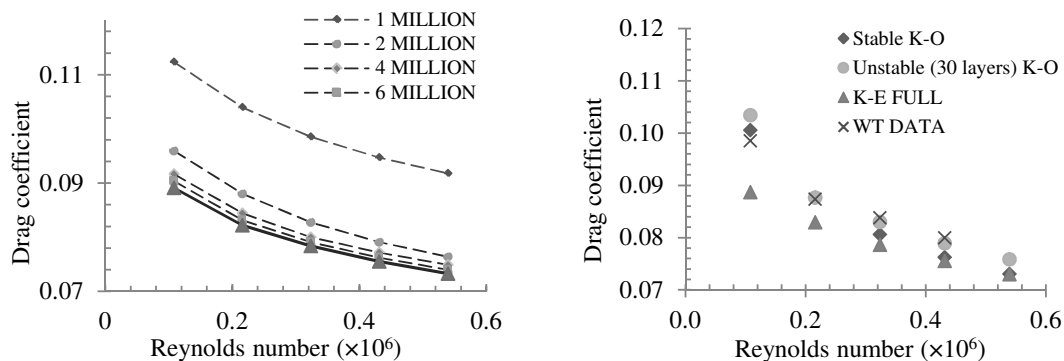


Fig. 3. (a) drag coefficient convergence characteristics; (b) drag coefficient variation with Reynolds number.

Apart from numerical data, the post analysis results were further studied to study the flow features around the simplified model. The flow features around the model are shown in Fig. 4 and Fig. 5. Fig. 4 shows the two main methods the simplified boxfish model achieves low drag characteristics. The front view indicates a transition of the inflow into four main regions; the unique shape allows transition into the back view with very little flow separation, which is mainly observed at the idealized mouth region, which was also found to be a region of improvement which may lead to lower  $C_D$ . The rear view indicates three vortices forming per side, which are generally not desirable, however, are shape specific. The main drag reduction from the back view is achieved through the diffusion process from all sides, which effectively contribute to the pressure recovery of the flow and reduce the  $C_D$ . Fig. 5(a) shows the flow characteristics of the airflow around the simplified model. Due to the sharp rear diffusion angle, flow



separation is inevitable, even for a  $Re$  number of  $0.1 \times 10^6$ . Fig. 5(b) shows the static pressure characteristics at a  $Re$  number of  $0.1 \times 10^6$ , similar to that of Fig. 5(a). It can be seen that regions of relatively high pressure exist near the idealized region as well as a diffusion region during which pressure recovery is occurring located at the rear of the simplified model.

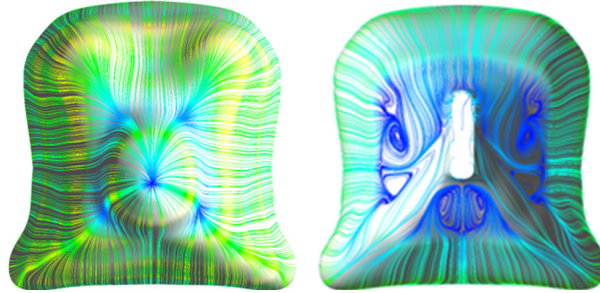


Fig. 4. surface streamline characteristics ( $k-\epsilon$ ): (a) front view; (b) rear view.

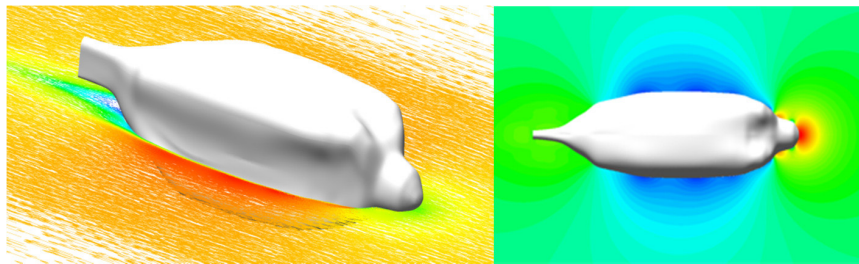


Fig. 5. (a) velocity vector for simplified model; (b) static pressure characteristics of simplified model.

#### 4. Conclusions

The drag characteristics of a simplified boxfish model were studied and it was found that a similar geometry to that of a boxfish has very favourable drag characteristics for such a bluff geometry. CFD has allowed the study of flow characteristics of the simplified model to be studied, together with currently available wind tunnel data and mesh convergence studies, confidence in the CFD results had been established, despite slight variation between the two standards:  $k-\omega$  and  $k-\epsilon$ , an overall agreement at higher Reynolds numbers was achieved. The simplified model displayed a favorable drag coefficient of 0.073 at a Reynolds numbers equivalent to 100 km/h inflow velocity. Boxfish geometry was found to be a very efficient at minimising the disturbance of flow through the tested medium.

#### References

- [1] S. Peter, J.H.K.S. Fiske, Lean, Light and Quiet: Advances in Automotive Energy Efficiency through Biomimetic Design. SAE International, SAE Technical Paper. (2008-21-0028).
- [2] M.P. Zari, Biomimetic approaches to architectural design for increased sustainability, School of architecture, Victoria University, NZ, 2007.
- [3] European Automobile Industry Report 2009/2010. ACEA: [www.acea.be](http://www.acea.be) [accessed on 10 December 2011].
- [4] W.H. Hucho, Aerodynamics of Road Vehicles, 4th ed., SAE International, USA, 1998.
- [5] H. H. Choi, H. Park, W. Sagong, Biomimetic flow control based on morphological features of living creatures, Physics of Fluids, 24 (2012) 121302.
- [6] J.E. Randal, Ostracion rhinorhynchus, Fishbase.org, [accessed on 10 December 2011]
- [7] F. Alam, G. Zimmer, S. Watkins, Mean and time-varying flow measurements on the surface of a family of idealized road vehicles, Experimental Thermal and Fluid Sciences. 27 (2003) 639-654.